Dynamics of proton spin-lattice relaxation in glycerol

E. Koivula, M. Punkkinen, W. H. Tanttila,* and E. E. Ylinen
Wihuri Physical Laboratory and Department of Physical Sciences, University of Turku, 20500 Turku 50, Finland
(Received 26 November 1984)

We have measured the temperature dependence of the proton spin-lattice relaxation time T_1 in glycerol in the temperature range 5—300 K. The lattice dynamics responsible for the relaxation in the range $5<T<160$ K is calculated using solitons with a formation energy $\Delta/k=1$ K. In the range $220<T<300$ K the dynamics of the lattice includes solitons with a formation energy $\Delta/k=4200$ K and these are used to calculate the relaxation of the protons. In both temperature ranges the heat capacity, thermal expansion, and heat conduction are calculated using the same parameters for the soliton representation as were used to calculate the temperature dependence of the proton spin-lattice relaxation time. Discontinuities in the thermal properties at the glass transition temperature T_g are attributed to an effective-mass change of the low-energy solitons. This work was conducted to test, with the use of nuclear magnetic resonance, some recent ideas in the dynamics of amorphous materials.

I. INTRODUCTION

The object of this work is to study the dynamics of amorphous material by measuring the nuclear-spin relaxation times of nuclei of the material. The nuclear magnetic moment and the nuclear quadrupole moment interact with the time-varying electromagnetic fields caused by thermal agitation in their vicinity.[1] This interaction brings about a change in the spin state of the atom. The characteristic time for a system of nuclear spins to attain thermal equilibrium with the lattice vibrations is called T_1. Recently, there have been studies of the temperature dependence of T_1 of quadrupolar nuclei[2] in amorphous materials and the results have been explained more or less successfully using the two-level system.[3] In fact much of the recent interest in T_1 measurements has actually been triggered by specific-heat measurements in glasses[4] and the analysis of the low-temperature specific heats in these materials.

In the two-level system an atomic quantity oscillates in a potential minimum separated from another higher relative minimum by a potential barrier. The atomic quantity can surmount the barrier and oscillate in the higher potential minimum and return to the lower potential minimum. The model has been popular because it has several parameters that can be adjusted, and one can use a spectrum of values for these parameters. The model has had good success[5] at least at low temperatures and must mirror some dynamical attribute of the physical system. There has been a good deal of speculation about what this attribute is.[5]

Work we have done[6] using molecular-dynamics computer simulations on Lennard-Jones two-dimensional solids indicates that large peninsulas of atoms projected into nonequilibrium static voids in the glassy material can wag at a relatively low frequency. These peninsulas can and do change their shapes, in which case the wagging frequencies change in response to the change of the moment of inertia of the peninsula. All this wagging-type motion happens at very low temperatures. Some atoms also move singly along the inside walls of the voids at low temperatures. At somewhat more elevated temperatures the voids shift around, which suggests that the theoretical description, first suggested by Takeno and Goda,[7] may be a correct description at higher temperatures. According to the above ideas the nuclear spin-lattice relaxation process in glasses at very low temperatures would be due to the two-level system and at higher temperatures would be due to excitations of the type suggested by Takeno and Goda.

Some significant support for the existence of localized low-density regions has been found in positron-annihilation studies in glassy materials.[8] This is not inconsistent with the Takeno-Goda theory. Also, MacKenzie[9] has discussed so-called prevacancy effects or dilatation effects in metals as found in numerous positron-annihilation studies. These dilatations are consistent with a model of excitations discussed by us.[10]

To study the dynamics of amorphous materials we selected glycerol as the material, primarily because it is rather easy to bring glycerol from a rather hard glass to a liquid by varying the temperature, the glass temperature being 193 K.[11] We measured as a function of temperature the proton relaxation times T_1 and T_{1D} for the Zeeman and dipolar energies, respectively. There was an added advantage in using glycerol in that other data[12] on the proton relaxation time T_1 exist in part of the temperature range so that we could compare our results with published results where applicable. Another advantage to using glycerol was that in the liquid state a well-accepted theory[13] of nuclear spin-lattice relaxation exists for nonquadrupolar nuclei such as protons. A serious disadvantage is that the relaxation process, if measureable at lower temperatures, must go through the intermediary of a paramagnetic impurity since proton-proton spin interactions are too small to relax the spins.[14] This complicated our analysis.

We believe that the dynamics in the amorphous state responsible for the nuclear spin-lattice relaxation is also

 ©1985 The American Physical Society

responsible for other thermal effects, such as thermal expansion, specific heat, and heat conduction, and we have calculated these quantities using parameters applied to the nuclear spin-lattice relaxation. For the proton spin-lattice relaxation it is not so important whether we talk about molecular reorientations without any connection to the lattice motion, or about reorientations related to dynamic density variations of glycerol, but the difference becomes evident when one considers the thermal properties mentioned above. We have used excitations of the Takeno-Goda type, but have taken the liberty of simplifying their use so that, in fact, the treatment resembles Landau's use of rotons in liquid helium. Our measurements were made at temperatures higher than those where we believe the two-level-system representation to be useful.

The balance of the work is divided into three parts. Section II is devoted to the experimental method and results. Section III is devoted to discussion of the results of the spin-lattice relaxation measurements as well as a discussion of other experimental thermal quantities. Section IV is devoted to conclusions.

II. EXPERIMENTAL

The glycerol sample used was supplied by Fluka AG and had a guaranteed water content of less than 0.1%. The sample was still dried under a vacuum at 90 °C for 6 h after which time the glass tube holding the glycerol was sealed under the existing vacuum.

After much experimentation a method was devised that gave reproducible values for our T_1 measurements. We found that different cooling rates and different initial temperatures would give us different glasses, and indeed this sort of result was supported by other workers.[15] The method we employed was to keep the glycerol sample at +50 °C for 30 min prior to cooling. During that time the sample was in the sample chamber within the liquid nitrogen in the cryostat. The sample was insulated from the nitrogen by a vacuum space and the temperature was maintained at +50 °C by a heater in the sample chamber. The cooling was initiated by turning off the heater and admitting helium gas into the vacuum space. The initial cooling rate that resulted at the sample was about 25 K/min and remained relatively high well below the glass transition temperature (193 K). A temperature of −160 °C was reached in about 10 min.

A Pt-resistance thermometer and the sample tube were located in the sample chamber which contained helium gas as a heat exchanger. There could have been some delay in the cooling of the sample relative to the cooling of the thermometer, but we believe this delay was slight, at least in the temperature range between room temperature and the glass transition temperature (193 K). The glass preparation outlined above was used daily so that the glass was never more than a day old.

The nuclear pulse spectrometer was a Bruker model SXP 4-100 operating at 35 MHz. The relaxation times T_1 were recorded using a 90°-τ-90° or n90°-τ-90° pulse sequences. The signal amplitudes corresponding to different intervals τ were fitted to an exponential function to obtain values for T_1. Below 50 K the amplitude of the free-induction signal at thermal equilibrium was extrapolated by using the observed amplitude at liquid-nitrogen temperature. After saturation the observed signal amplitude seems to grow exponentially with time toward the extrapolated value. The measured T_1 values at 15 and 30 K are based on actual measured thermal-equilibrium signals. Our data agree very well with those of Kintzinger and Zeidler.[12] We thus have the reassurance that our data are reliable.

III. DISCUSSION

The results of the T_1 and T_{1D} measurements are shown in Fig. 1 for high temperatures and in Fig. 2 for low temperatures. The main features of the data that we will concentrate on are the temperature dependences of T_1 in both the high-temperature range and the low-temperature range. We believe that the relaxation processes in these two temperature ranges result from two fundamentally different processes and we will discuss them separately. The relaxation process in the high-temperature range results from the magnetic dipole-dipole interaction between the protons, whereas in the low-temperature regime the relaxation is via paramagnetic impurities which are relaxed by thermal processes and, in turn, which relax the protons.

A. Spin relaxation in the high-temperature range

The temperature dependence of the relaxation time T_1 is given in Fig. 1. For glycerol, the glass transition temperature is 193 K and the minimum in T_1, shown in Fig. 1, is at 283 K, well above the glass transition temperature. We assume that the relaxation time T_1 is due to thermal rotational motions of the glycerol molecules in the liquid and is given by[16]

$$\frac{1}{T_1}=C\left[\frac{\tau_c}{1+\omega^2\tau_c^2}+\frac{4\tau_c}{1+4\omega^2\tau_c^2}\right], \tag{1}$$

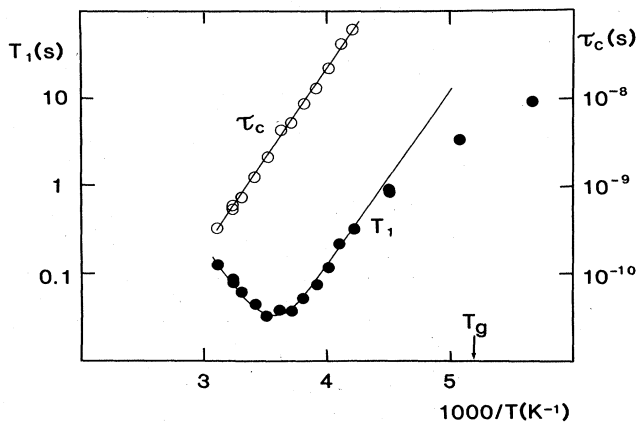

FIG. 1. Logarithm of the spin-lattice relaxation time T_1 of protons in glycerol as a function of $1000/T$. Also shown is the correlation time τ_c [see Eq. (1)] in the same temperature interval. The glass transition temperature (193 K) is also shown.

where C is a constant, τ_c is the correlation time for the thermal motion, and ω is the Larmor angular precession frequency of the proton nuclear spins. A maximum exists for the above function when $\omega\tau_c \equiv 0.616$. For $\omega = 2\pi(35\times10^6)$ we get $\tau_c = 2.8\times10^{-9}$ s at the T_1 minimum. The measured value for the T_1 minimum is 32.9 ms at 285.2 K. Solving for C we get $C = 4.7\times10^{+9}$. For other measured T_1's one can now solve for the correlation time as a function of the temperature if one so desires.[1]

Over the range 322.4—243.9 K the natural logarithm of the correlation time τ_c is represented by a linear function of $1/T$ as shown in Fig. 1. According to Debye,[16]

$$\tau = 3\tau_c = 4\pi\eta\alpha^3/k_BT \ , \tag{2}$$

where η is the viscosity, α is a hard-sphere molecular radius, and k_B is Boltzmann's constant. Taking the logarithm of Eq. (2), we get

$$\log_{10}\tau = K + \log_{10}(\eta/T) \ . \tag{3}$$

If one plots $\log_{10}(\eta/T)$ vs $1/T$ using measured values of η at various temperatures,[17] one does get a linear dependence. However, this plot corresponds to an activation energy of about 17 kcal/mol, which is significantly higher than that obtained for τ_c from our T_1 data. Bloembergen, Purcell, and Pound[13] assumed a linear relation between τ_c and η/T. Our results, shown in Fig. 1, yield $\tau_c \propto (\eta/T)^{0.57}$ rather than the linear result $\tau_c \propto \eta/T$ of Bloembergen, Purcell, and Pound. We have confidence in our T_1 data since they agree with those of Kintzinger and Zeidler.[12]

Torrey[18] has suggested a dependence for τ_c of the form

$$\tau_c = \tau_0 e^{E/k_BT} \ . \tag{4}$$

This equation, with $E = 9.57$ kcal/mol, gives a good fit to our experimental data for T_1. This expression comes from a physical situation in which an atom has to surmount a barrier of height E to make a successful jump or rotation. We criticize this physical process using the following argument. The measured value for τ_c is about 10^{-9} s at the T_1 minimum. For $E = 9.57$ kcal/mol, also measured, it is required that $\tau_0 \simeq 10^{-16}$ s. The attempt frequency for this sort of *activated process* is $f_0 \simeq 1/\tau_0 = 10^{16}$ s^{-1}. This frequency is much higher than any frequency available to the molecules in the glycerol, it being considerably above optical frequencies. The temperature range of 244—322 K is rather short, but even then the experimental errors do not allow a large enough reduction in f_0. In some cases the prefactor τ_0 is not a well-defined quantity. A gradual change in the type of the motion, for instance, invalidates the picture of activated rotations over a defined barrier and an anomalous τ_0 will be observed. A distribution of correlation times can change the factor τ_0, but cannot explain the short value around the T_1 minimum. It seems to us that the applicable correlation time τ_c cannot have its origin in an activated diffusion or activated rotation over a fixed barrier.

We believe that the molecular rotation is responsible for the nuclear spin-lattice relaxation. We have shown that the Debye relaxation is applicable at the higher temperatures. We must now account for the correlation time τ_c of the molecular rotation. It has been shown[19] that a considerable number of lattice vibrational states are missing in amorphous materials. The loss of these states would normally imply a reduction in the heat capacity of glasses. The heat capacities of amorphous materials are, however, most often higher than they "should" be and often exceed the Dulong-Petit limit. The clear implication is that some type of excitation other than the harmonic lattice vibration *must* be present in the amorphous material. These excitations are not of minor importance, but are of comparable importance to the harmonic lattice vibrations. This type of excitation was first introduced by Takeno and Goda[7] to explain the low-temperature specific heat of some glasses. Later we independently suggested[7] excitations of the Takeno-Goda type and applied the results to the specific heat of amorphous materials over a large range of temperatures. Watkins and Fenichel[20] have shown that the model we suggested was not directly applicable to amorphous materials at very low temperatures. The model of Takeno and Goda and our model are ambiguous to some extent; Takeno and Goda's because of several adjustable parameters with very little insight into the physical meaning of the parameters, ours essentially for the same reason, but with even less insight into the precise form of the excitations. Yet, excitations such as those of Takeno and Goda and ourselves have been used with perhaps less justification than we are presenting. A case in point are Landau rotons, which were, at their inception, somewhat vague quantities. Theories of nonlinear excitations in one-dimensional systems[21] have advanced quite far. The theory of nonlinear excitations in two- and three-dimensional media is essentially nonexistent. In computer simulations,[22] however, one can see definite nonlinear effects, such as the formation of voids and translations of low-density entities quite similar to what we have in mind. In the present case as stated in the Introduction, we performed T_1 measurements on protons in glycerol to seek support for the existence of these excitations. The compulsion that we felt in introducing them came from numerous other physical attributes of amorphous materials, such as, for example, the melting phenomenon. Another of these phenomena[23] is the increase in the positron lifetimes in amorphous material, such as liquids, upon expansion of the amorphous materials with an increase in temperature. It is quite generally held[24] that the positronium atom is trapped in localized voids or low-density regions in the amorphous material. Either the number or the size of the voids, or both, increase with temperature, thereby increasing the positron lifetime. The decrease in electron density in the low-density region decreases the positron-electron—annihilation rate for the ortho positronium.[25] The problem with the positron-annihilation work is that so far it has not been shown that the low-density regions that are presumed to be present are, in fact, in motion. We are currently designing positron-annihilation experiments[26] that will determine whether or not the low-density regions are in motion.

The soliton description is not the only model for explaining the relaxation. Actually, the concept of thermal-

ly activated reorientations has been used at high temperatures. However, we introduced solitons to be able to use the same model of motion to explain other thermal properties and to explain the relaxation at low temperatures. The physical process responsible for nuclear spin-lattice relaxation which we propose to be taking place is one in which an excitation, which we choose to call a soliton, passes through the atom on which we are focusing our attention. The soliton, while passing through the atom, causes the atom to move relative to its neighbors and we postulate that it is the agent responsible for the rotation. Since a single collision is likely to cause only a small angular displacement of the concerned molecule relative to the neighbors, and since the rotation necessary to cause a significant change in magnetic interaction is of the order of a radian, the correlation time will be some multiple of the average time between collisions of solitons with a particular molecule.

For the purpose of making calculations we have made the following assumptions:

(1) The solitons are freely moving low-density regions within the sample which have thermal kinetic energies.

(2) The fraction of the volume taken up by the solitons should not exceed the sample volume.

(3) The size (radius) of the solitons is temperature independent, as is the effective mass.

(4) The lower bound for the size of the solitons is determined by the fact that they should include several molecules.

(5) Despite the fact that the speed of the solitons must be less than the speed of sound, we have ignored this in many cases for calculational convenience, where the error introduced is small.

(6) We have used Maxwell-Boltzmann statistics, again for calculational convenience, despite the fact that it introduces some error, and though we feel the correct statistics should be of the Bose-Einstein type.

The average time between collisions of solitons with a molecule is calculated in the approximation in which the density of solitons is low. Let τ be the time of collision ($=2R/v$), τ' the time between collisions, R the radius of the soliton, v the average velocity of the soliton, V the volume of a soliton, V_0 the sample volume, N the total number of solitons, n the number density of solitons, Δ the soliton formation energy, and m^* the effective dynamical soliton mass. On the average,

$$\frac{\tau}{\tau'}=\frac{NV}{V_0}=nV, \quad \tau'=\frac{\tau}{nV}=\frac{2R}{vnV} . \tag{5}$$

Now we assume

$$n=\left[\frac{m^*k_BT}{2\pi\hbar^2}\right]^{3/2} e^{-\Delta/k_BT}, \tag{6}$$

$$v=\left[\frac{2k_BT}{m^*}\right]^{1/2} . \tag{7}$$

Using (6) and (7) in (5), we get

$$\tau_c=\tau'=\frac{\tau_0}{T^2}e^{\Delta/k_BT} , \tag{8}$$

where

$$\tau_0=\frac{Rh^3}{2\pi^{3/2}k_B^2Vm^*}=\frac{3h^3}{8\pi^{5/2}k_B^2R^2m^*} . \tag{9}$$

Equation (8) is fitted to the measured values shown in Fig. 1 (smooth curve). The fitted values are $\tau_0=6.4\times10^{-11}$ s K^2 and $\Delta=8.41$ kcal/mol.

The two parameters R and m^* must have the product value $R^2m^*=5.12\times10^{-46}$ m^{2}kg in order that $\tau_0=6.4\times10^{-11}$ s K^2. We have tabulated in Table I various values of R and m^* that satisfy the required value of R^2m^*. The values $R=5$ Å and $m^*=2.05\times10^{-27}$ kg lie close to what we might consider to be reasonable values; however, as mentioned earlier, numerous collisions are required to produce a significant molecular rotation, so that the correlation time τ_c is significantly longer than the time between collisions, τ'. We shall find later that it is possible to explain T_1 as well as other thermal properties if we assume $\tau_c=48\tau'$, $m^*=5.8\times10^{-26}$ kg, and $R=6.5$ Å.

B. Spin relaxation in the low-temperature region

For the relaxation-time dependence on the temperature at low temperatures ($4<T<150$ K) we also present a soliton description. However, in this case we consider the relaxation process to be different. The nuclear relaxation at low temperatures is no longer governed by reorientations, but rather by paramagnetic impurities. The spin motion of paramagnetic impurities is then related to motion, which we describe in terms of solitons.

If the relaxation took place via magnetic dipolar interaction between protons, then in the slow-motion case $\omega_0\tau\gg\Delta\omega\tau\gg1$ the ratio T_1/T_{1D} would be approximately

$$\frac{T_1}{T_{1D}}=\frac{C'[\tau/(1+\Delta\omega^2\tau^2)]}{C[\tau/(1+\omega_0^2\tau^2)]}\approx\left[\frac{\omega_0}{\Delta\omega}\right]^2 .$$

Here C and C' are nearly equal and $\Delta\omega/\gamma$ would be of the order of a few gauss. This would give, in our case of

$\omega_0/\gamma=8000$ G,

$$T_1/T_{1D}\approx10^6 .$$

TABLE I. Nominally allowed values of the radius R of a soliton and the dynamical mass m^* of a soliton in glycerol.

R (Å)	m^* (kg)
1	5.12×10^{-26}
2	1.28×10^{-26}
5	2.05×10^{-27}
10	5.12×10^{-28}

This ratio is much larger than the observed ratio 10^3 below 150 K. For this reason we believe that paramagnetic impurities are responsible for the relaxation. The relaxation was exponential at all temperatures, so that we will assume fast spin diffusion outside a spin-diffusion barrier $r > b$.[27] There is no spin diffusion inside a sphere of radius b surrounding the impurity. The paramagnetic impurity concentration in our sample as determined by paramagnetic resonance was less than 2×10^{-6} molar fraction.[28] In this case we have approximately

$$\frac{1}{T_1}=\frac{C}{b^3}\frac{\tau}{1+\omega_0^2\tau^2},$$

$$\frac{1}{T_{1D}}=\frac{C'}{b'^3}\frac{\tau}{1+\Delta\omega^2\tau^2}.$$

Here C and C' are proportional to the concentration of the paramagnetic ions but are otherwise nearly equal. The spin-diffusion barrier b' for the dipolar energy may differ from b. Usually in the case of the relaxation via paramagnetic centers, τ is taken to be equal to the spin-lattice relaxation time of the paramagnetic spins.

The spin-lattice relaxation is dominated by the interaction between the paramagnetic ion and those protons, which are situated just outside b or b'. For those protons the resonance shift, and also the change of the dipolar energy, is

$$\Delta\omega\approx\mu_e/b'^3,$$

where μ_e is the electronic magnetic moment. In the case of long correlation time $\omega_0\tau\gg\Delta\omega\tau\gg1$, we have roughly

$$\frac{T_1}{T_{1D}}\approx\frac{C'}{C}\left[\frac{b}{b'}\right]^3\left[\frac{\omega_0}{\Delta\omega}\right]^2\approx\frac{\omega_0^2}{\mu_e^2}b^3b'^3.$$

It should be possible to choose b and b' such that the experimentally observed ratio $T_1/T_{1D}=10^3$ is reproduced.

The above reasoning was aimed at demonstrating that the low-temperature relaxation is really governed by paramagnetic impurities. The same conclusion is obtained even if the T_{1D} process, being the faster of the two relaxation processes, was in the diffusion-limited region. Then the T_{1D} values should be longer than in the presence of rapid spin diffusion. This would make the ratio $T_1/T_{1D}\simeq10^3$ even easier to explain.

Electron paramagnetic impurity spins are relaxed via the spin-orbit interaction. The Stark effect couples the orbital motion to the thermal motion of the lattice.[29] The relevant lattice motions are related to the passage of solitons through the paramagnetic impurities. The electron spin flips and the resulting perturbation at the neighboring nuclei flips the nuclear spins, followed by nuclear spin diffusion. The relevant time here is the time during which the soliton passes through the paramagnetic impurity. When a soliton arrives at the impurity the perturbation is switched on, and when the soliton departs from the impurity the perturbation is switched off. This is exactly the same as in spin-rotation interaction and the same correlation function will be used. Brown *et al.*[30] show that a reasonable correlation function for this process is

$$G(t)=\begin{cases}\frac{\tau}{\tau'}e^{-\tau/\tau'}\frac{\tau-|t|}{\tau}, & |t|<\tau\\ 0, & |t|>\tau.\end{cases}\tag{10}$$

The Fourier transform of $G(t)$ is

$$J(\omega)=\frac{\tau}{\tau'}e^{-\tau/\tau'}\int_0^\tau\cos(\omega t)\left[\frac{\tau-t}{\tau}\right]dt$$

$$=\frac{\tau}{\tau'}e^{-\tau/\tau'}\{[1-\cos(\omega\tau)]/\omega^2\tau\}.\tag{11}$$

Now for $\omega=2\pi\times35\times10^9\ \mathrm{s}^{-1}$ and the temperature range 4–160 K, one has $\tau\approx10^{-13}$ and $\omega\tau\approx10^{-2}$. We can expand $\cos(\omega t)$ retaining terms to second order:

$$J(\omega)=\frac{1}{2}\frac{\tau^2}{\tau'}e^{-\tau/\tau'}=\tfrac{1}{2}\tau nVe^{-nV}$$

$$=R\left[\frac{m^*}{2k_BT}\right]^{1/2}\left[\frac{m^*k_BT}{2\pi\hbar^2}\right]^{3/2}e^{-\Delta/k_BT}e^{-nV}.\tag{12}$$

The temperature dependence of this function is

$$J(\omega)\propto ATe^{-\Delta/k_BT}e^{-n(T)V}.\tag{13}$$

The transition probability for an electron spin flip W is proportional to $J(\omega=2\pi\times35\times10^9)$. The relaxation time $T_1=2/W$ is plotted in Fig. 2 as a solid line in the lowest-temperature range with $\Delta/k_B=1$ K, $m^*=10^{-27}$ kg, and $R=1$ Å. We emphasize that even though the terms we use in the low-temperature–regime derivation *have the same symbols* as in the high-temperature regime, *the solitons are different.*

To explain the temperature dependence of T_1 in the range 60–160 K we shall use a Raman (indirect) process. For this derivation we will need the density of occupied soliton states at an energy E. For solitons, considered as free particles, we have

$$N(v)=\frac{4\pi}{h^3}m^{*3}e^{-\Delta/k_BT}e^{-m^*v^2/2k_BT}v^2,\tag{14}$$

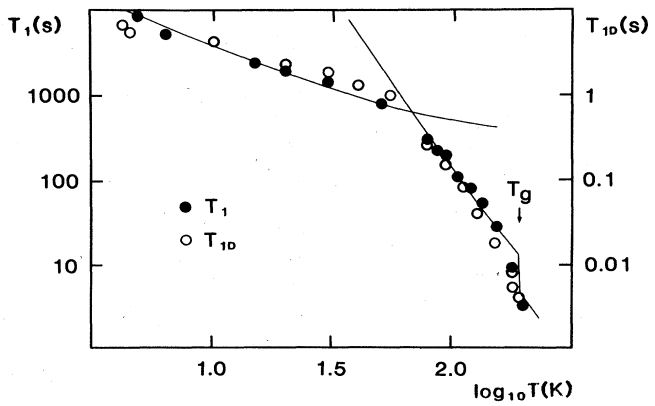

FIG. 2. Experimental relaxation-time points and theoretical curves. Lower-temperature range is due to a direct process, higher-temperature range to an indirect process. T_1 is denoted by solid circles and T_{1D} by open circles.

where $N(v)$ is the number of solitons per unit volume in a unit velocity range; that is, $N(v)dv$ is the numer of solitons per unit volume between v and $v+dv$. One gets, from Eq. (14),

$$N(E)=4\pi\sqrt{2}\left[\frac{m^*}{h^2}\right]^{3/2}e^{-\Delta/k_BT}e^{-E/k_BT}\sqrt{E}\ , \qquad (15)$$

$$E=\tfrac{1}{2}m^*v^2\ \ (E<m^*c^2)\ ,$$

where $N(E)dE$ is the number of solitons per unit volume in the range between E and $E+dE$.

The model has the solitons scattered inelastically by the electron spins via the spin-orbit coupling and the Stark effect.[29] The matrix element involved in this interaction is proportional to the products of the incident- and scattered-soliton energies as well as by the products of the densities of solitons at those energies integrated over all allowed scattering processes:[31]

$$\frac{1}{T_1}\propto\int_0^\infty E(E+E_0)N(E)N(E+E_0)dE\ , \qquad (16)$$

where $E_0=h\nu_0=k_BT_0$ is the electron-spin transition energy and $T_0=1.68$ K at the magnetic field used. We restrict the upper limit on the integral:

$$\frac{1}{T_1}\propto 32\pi^2\left[\frac{m^*}{h^2}\right]^3\exp(-2\Delta/k_BT)\times\int_0^{E_{\max}-E_0}\exp[-(2E+E_0)/k_BT]\times E(E+E_0)\sqrt{E}\,(E+E_0)^{1/2}dE\ ,$$

where

$$E_{\max}=\tfrac{1}{2}m^*c^2\ . \qquad (17)$$

Now since a typical kinetic energy $E_{\rm typ}$ of solitons at temperature T is k_BT,

$$\frac{E_{\rm typ}}{E_0}=\frac{T}{T_0}\gg 1\ . \qquad (18)$$

We can approximate Eq. (17) as follows:

$$\frac{1}{T_1}\propto 32\pi^2\left[\frac{m^*}{h^2}\right]^3\exp\left[-\frac{2\Delta+E_0}{k_BT}\right]\times\int_0^{E_{\max}}E^3\exp(-2E/k_BT)dE\ . \qquad (19)$$

Denoting $\Theta=E_{\max}/k_B$, the relevant temperature dependence of Eq. (19) can be expressed as

$$\frac{1}{T_1}\propto\exp\left[-\frac{2\Delta+E_0}{k_BT}\right]\left\{6\left[\frac{T}{2}\right]^4-\exp(-2\Theta/T)\times\left[\Theta^3\frac{T}{2}+3\Theta^2\left[\frac{T}{2}\right]^2+6\Theta\left[\frac{T}{2}\right]^3+6\left[\frac{T}{2}\right]^4\right]\right\}\ . \qquad (20)$$

In the temperature range $(2\Delta+E_0)/k_B<T<\Theta$, Eq. (20) gives, in an approximation $1/T_1\propto T^4$, but a slower dependence on T for $T>\Theta$. Using $m^*=10^{-27}$ kg, $\Delta/k_B=1$ K, and $R=1$ Å gives the continuous curve in the higher-temperature range in Fig. 2. There is a discontinuity shown at the glass transition temperature, and this will be discussed later. These are the same values that were used for the direct process in the lower-temperature range in Fig. 2 ($4<T<60$ K).

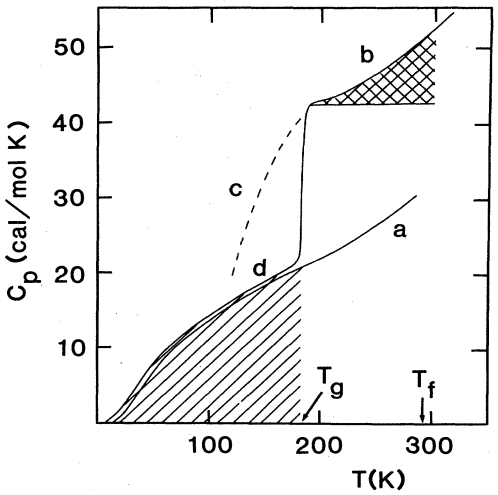

FIG. 3. Molar heat capacity of glycerol as a function of temperature (Ref. 11). The shading has been added by us. *a*, crystal; *b*, melt; *c*, melt cooled very slowly; *d*, glass.

C. Other thermal properties

We will first discuss the molar heat capacity of glycerol as shown in Fig. 3. At the glass transition temperature the molar heat capacity makes an extremely rapid jump of about 20 cal/mol K. We will discuss this jump later, and at this time we will consider only the contribution to the molar heat capacity above the glass transition temperature T_g in the cross-hatched region shown in Fig. 3. The molar-heat-capacity contribution at 300 K in the cross-hatched region is 10 cal/mol K. We attribute this to the solitons with a formation energy, deduced from T_1 measurements and Eq. (8), of

$$\frac{\Delta}{k_B}=4200\ \text{K},\quad \Delta=8.41\ \text{kcal/mol}\ .$$

The molar heat capacity is

$$C_p\approx C_V=\frac{dN}{dT}(\tfrac{3}{2}k_BT+\Delta)+\tfrac{3}{2}Nk_B=k_BV_0\left[\frac{2\pi m^*k_BT}{h^2}\right]^{3/2}\times e^{-\Delta/k_BT}\left[\left[\frac{3}{2}+\frac{\Delta}{k_BT}\right]^2+\tfrac{3}{2}\right]\ , \qquad (21)$$

where N is the number of solitons per mole and $V_0=7.1\times10^{-5}$ m^3 is the molar volume. From this expression, using $C_p=10$ cal/mol K, $T=300$ K, and $\Delta/k_B=4200$ K, we get

$$m^*=5.8\times10^{-26}\ \text{kg}=35m_p$$

for the soliton mass, where m_p is the proton mass.

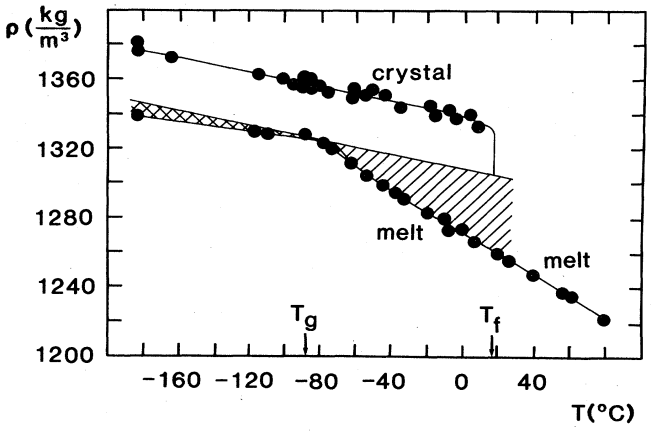

FIG. 4. Density of glycerol as a function of temperature (Ref. 11). The upper line tangential to the glass curve as well as shading has been added by us.

Now we will examine that part of the thermal expansion which is in excess of the expansion of crystalline glycerol and is shown in Fig. 4 as a shaded area above T_g. We will solve for V (the volume of a soliton) and ρ (the soliton mass density). For this we require the following two equations:[32]

$$\frac{m^*}{V}=\rho\left[\frac{\rho_0-\rho}{\rho}\right]^2, \tag{22}$$

where ρ is the density inside the solitons and ρ_0 is the density of the glass in absence of solitons, and

$$\rho'=(1-nV)\rho_0+nV\rho\ , \tag{23}$$

where ρ' is the glass density at $T=300$ K. The soliton number density can be calculated using Eq. (6) to be $n(T=300\text{ K})=1.68\times10^{26}$ m^{-3} using $\Delta/k_B=4200$ K and $m^*=5.8\times10^{-26}$ kg. Using the values from Fig. 4, $\rho_0=1305$ kg m^{-3} and $\rho'=1260$ kg m^{-3} at 300 K, we get

$$V=\frac{[(\rho_0-\rho')^2/n]+m^*(\rho_0-\rho')}{m^*n\rho_0}=1.16\times10^{-27}\text{ m}^3\ ,$$

$$R=6.52\text{ Å}\ ,$$

$$nV=0.194\ .$$

Now we can solve for ρ,

$$\rho=\frac{\rho'-(1-nV)\rho_0}{nV}=1070\text{ kg m}^{-3}\ ,$$

$$\rho/\rho_0=0.822\ .$$

Now we note that m^*R^2 is considerably greater than the value of 5.12×10^{-46} m^{2}kg used in calculating the values for Table I. In using 5.12×10^{-46} m^{2}kg we assumed that every collision produced a significant rotation of the glycerol molecule. Now we must assume that

$$(5.8\times10^{-26})(6.52\times10^{-10})^2/5.12\times10^{-46}=48.2$$

collisions are required to produce a significant molecular rotation, or that the correlation time is 48 times longer than the collision time. This seems to us to be a reasonable result.

We now examine the low-temperature thermal properties which we postulate to be due to the same solitons that caused the low-temperature spin-lattice relaxation. These solitons have a formation energy

$$\Delta/k_B\approx1\text{ K}\ .$$

We will choose the effective mass m^* so that the heat capacity of quenched glass (shaded area in Fig. 3) will have the measured value at T_g. In this calculation we restrict the momentum to be less than m^*c, where $c=3.61\times10^3$ m s^{-1} since a large error would be incurred by allowing momenta above this value. We get

$$m^*\approx4.5\times10^{-28}\text{ kg}\ .$$

We attribute the sharp rise in the heat capacity to a sudden change of this m^* near T_g:

$$m^*\approx4.5\times10^{-28}\text{ kg},\quad T\lesssim T_g$$

$$m^*=6.0\times10^{-28}\text{ kg},\quad T\gtrsim T_g\ .$$

So far this rapid change in the heat capacity at T_g has not been explained using other theories, and the mass change of these light solitons is sufficient to explain the specific-heat discontinuity. The corresponding effect, calculated using Eqs. (19) and (20) and shown in Fig. 2, actually improves the agreement between the T_1 data and our calculations.

From Fig. 4 we see that if we attribute to the glassy glycerol a density change equal to that of crystalline glycerol as the temperature is changed at temperatures below T_g, plus a density change of its own, then there is actually a contraction contribution coming from the light-mass solitons.[33]

The number density of light-mass solitons can be calculated at T_g using the lighter effective mass, $m^*=4.5\times10^{-28}$ kg. One gets

$$n=\frac{2\pi}{h^3}\int_0^{m^*c}\exp\left[-\left[\frac{p^2/2m+\Delta}{k_BT}\right]\right]\rho^2dp$$

$$=3.346\times10^{28}\text{ m}^{-3}\ , \tag{24}$$

which gives, for one mole of glycerol,

$$N(T_g)=2.38\times10^{24}=4A\ ,$$

where A is Avogadro's number. Since there are 14 atoms per molecule of glycerol, the total number of terms in the Hamiltonian contributing to the specific heat have not been "used up." We can use Eq. (23) to fit the experimental density below T_g, shown as a cross-hatched area in Fig. 4. A variety of choices of the parameters give reasonable fits to the T_1 data as well as to the density.

TABLE II. Theoretical values of the molar heat capacity and the heat conductivity along with the experimental values of the heat conductivity of glycerol on either side of the glass transition temperature T_g.

m^* (kg)	C_p (cal/mol K)	K (cal/K m s)	K(Expt.)
4.5×10^{-28}	21	0.038	0.04
6.0×10^{-28}	42	0.066	0.06

TABLE III. Summary of the soliton parameters m^*, Δ/k_B, and R used in the various cases (ns denotes those values not specified).

	Temperature	m^* (kg)	Δ/k_B (K)	R (Å)
Heat capacity	$T=300$ K	5.8×10^{-26}	4200	ns
Thermal expansion	$T>T_g$	5.8×10^{-26}	4200	6.5
Relaxation	$T>230$ K	5.8×10^{-26}[a]	4200	6.5[a]
Heat capacity	$T<T_g$	4.5×10^{-28}	1	ns
	$T=T_g$	6.0×10^{-28}	1	ns
Thermal expansion	90 K $<T<T_g$	4.5×10^{-28}	1	1.2
Relaxation	$T<160$ K	10^{-27}	1	1

[a]Assumed: $\tau_c=48$ collision intervals.

The relevant parameters are R and m^*, which range in value from 1 to 1.4 Å and from 4.5×10^{-28} to 2.6×10^{-28} kg, respectively. Above T_g the number of low-temperature solitons is assumed to be constant, and they actually form the background for the high-temperature solitons. In any case a constant number, $14A$, of light-mass solitons will give the free-molecule classical limit of 14×3 cal$=42$ cal for the heat capacity. The heat capacity can increase above this value, however, since the molecules are bound and, as discussed earlier, the increase in the heat capacity above T_g is due to the addition of the heavy-mass solitons.

Additionally, the rapid increase in thermal conductivity at T_g with increasing temperature[11] can be explained reasonably well assuming the change in m^* near T_g and using the simple gaseous conduction equation

$$K=\tfrac{1}{3}(1.128)l\left[\frac{2k_BT}{m^*}\right]^{1/2}\frac{1}{V_0}C_p\ , \tag{25}$$

where $(2k_BT/m^*)^{1/2}$ is the mean thermal speed of solitons and $V_0=7.1\times10^{-5}$ m^3 is the molar volume. Using the collision distance $l=1$ Å we get the results shown in Table II. The value of 1 Å for the collision length seems rather short, but otherwise the results are consistent with our assumption of an effective-mass increase upon passing from temperatures immediately below T_g to temperatures immediately above T_g. Some of the results of the calculations are summarized in Table III; however, the results are more completely exhibited in Figs. 1–4.

IV. CONCLUSIONS

The spin-lattice relaxation time can be reconciled using the soliton representation. Unfortunately we have had to use two different sets of solitons. We have tried to insist that the same parameters used to rationalize the spin-lattice relaxation measurements also explain other thermal properties of the glycerol, such as the heat capacity, the thermal conductivity, and the thermal expansion. The results seem encouraging to us despite the fact that we have had to use—below the glass transition temperature—two parameters, namely the radius of a soliton, R, and the collision length of a soliton, l, which both seem to be rather short. The values of both R and l used that best fit the experimental data are 1 Å each. We would prefer to have them be several angstrom units each. Fits using several angstrom units are not bad but are not optimum.

We have offered no physical reason for representing the glass transition as a point at which the effective soliton mass changes. This change in the effective soliton mass was postulated only because it explained the changes in the various thermal quantities. Not only does this postulate require further investigation, but the soliton postulate itself also certainly does. There seems to be no question that the lattice wave picture is invalid in the wavelength region where the defects have the spacing of the wavelength of the lattice waves.

We made no attempt to explain our experimental results using the two-level system. As mentioned earlier the two-level system may have its greatest applicability at low temperatures ($T<2$ K), and becomes increasingly awkward to use as the temperature is raised. It is of interest to speculate as to the conditions under which a massless phonon becomes a massive soliton. These sorts of problems are probably related to the problems of high-energy physics.

ACKNOWLEDGMENT

One of us (W.H.T.) would like to thank the National Academy of Sciences of Finland for financial support.

*Permanent address: Department of Physics, University of Colorado, Boulder, CO 80309.

[1]See, for example, A. Abragam, *The Principles of Nuclear Magnetism* (Clarendon, Oxford, 1961).

[2]J. Szeftel and H. Alloul, J. Non-Cryst. Solids. **29**, 253 (1978); M. Rubinstein, H. A. Resing, T. L. Reinecke, and K. L. Ngai, Phys. Rev. Lett. **34**, 1444 (1976); M. Rubinstein and H. A. Resing, Phys. Rev. B **13**, 959 (1976); S. G. Greenbaum, U. Strom, and M. Rubinstein, *ibid.* **26**, 5226 (1982).

[3]W. A. Phillips, J. Low Temp. Phys. **7**, 351 (1972); P. W. Anderson, B. I. Halperin, and C. M. Varma, Philos. Mag. **25**, 1 (1972).

[4]R. B. Stephens, Phys. Rev. B **13**, 852, (1976); J. C. Lasjaunias, J. Non-Cryst. Solids **54**, 183 (1983).

[5]W. A. Phillips, J. Non-Cryst. Solids **31**, 267 (1978).

[6]D. J. Toms and W. H. Tanttila (unpublished).

[7]S. Takeno and M. Goda, Prog. Theor. Phys. **48**, 1468 (1972); W. H. Tanttila, Phys. Rev. Lett. **39**, 554 (1977).

[8]R. K. Wilson, P. O. Johnson, and R. Stump, Phys. Rev. **129**, 2091 (1963); R. L. de Zafra and W. T. Joyner, *ibid.* **112**, 19

(1958); W. Brandt, S. Berko, and W. W. Walker, *ibid.* **120**, 1289 (1960). For applications of positron-annihilation studies to condensed matter, see *Positrons in Solids,* edited by P. Hautojärvi (Springer, Berlin, 1979); *Positron Annihilation,* proceedings of the 6th International Conference on Positron Annihilation at the University of Texas at Arlington, 1982 edited by P. Coleman, S. Sharma, and L. Diana (North-Holland, Amsterdam, 1982); Philip R. Wallace, in *Solid State Physics,* edited by F. Seitz and D. Turnbull (Academic, New York, 1960), Vol. 10.

[9]I. K. MacKenzie, in *Positron Annihilation,* Ref. 8, p. 179.

[10]W. H. Tanttila, Phys. Status Solidi B **86**, K175 (1978); D. J. Toms and W. H. Tanttila, *ibid.* **102**, K101 (1980).

[11]A. R. Ubbelohde, *Melting and Crystal Structure* (Clarendon, Oxford, 1965).

[12]J. P. Kintzinger and M. D. Zeidler, Ber. Bunsenges. Phys. Chem. **77**, 98 (1973).

[13]N. Bloembergen, E. M. Purcell, and R. V. Pound, Phys. Rev. **73**, 679 (1948); H. C. Torrey, *ibid.* **92**, 962 (1953). See also *The Principles of Nuclear Magnetism,* Ref. 1, Chap. VIII.

[14]I. Waller, Z. Phys. **79**, 370 (1932).

[15]R. Calemczuk, R. Lagnier, and E. Bonjour, J. Non-Cryst. Solids **34**, 149 (1979).

[16]*The Principles of Nuclear Magnetism,* Ref. 1, p. 300.

[17]C. S. Miner and N. N. Dalton, *Glycerol* (Reinhold, New York, 1953), pp. 281 and 284; H. Hausdörfer, in *Ullmanns Encyklopädie der technischen Chemie,* edited by H. Buchholz-Meisenheimer (Urban and Schwarzenberg, München, 1957), Vol. 8 p. 194; *CRC Handbook of Chemistry and Physics,* edited by R. Weast (Chemical Rubber Co., Cleveland, 1971).

[18]H. C. Torrey, Phys. Rev. **92**, 962 (1953).

[19]W. A. Phillips, J. Non-Cryst. Solids **31**, 267 (1978).

[20]G. M. Watkins and H. Fenichel, J. Non-Cryst. Solids **37**, 433 (1980).

[21]See, for example R. K. Dodd, J. C. Eilbeck, J. D. Gibbon, and H. C. Morris, *Solitons and Nonlinear Wave Equations* (Academic, New York, 1982), or P. G. Drazin, *Solitons* (Cambridge University Press, New York, 1983), or G. L. Lamb, *Elements of Soliton Theory* (Wiley, New York, 1980).

[22]S. Toxvaerd, Phys. Rev. Lett. **44**, 1002 (1980); R. M. J. Cotterill *ibid.* **42**, 1541 (1979); D. J. Toms and W. H. Tanttila (unpublished).

[23]R. K. Wilson, P. O. Johnson, and R. Stump. Phys. Rev. **129**, 2091 (1963).

[24]Nobuhiro Shiotani, in *Positron Annihilation,* Ref. 8, p. 561.

[25]P. Hautojärvi and A. Vehanen, in *Positrons in Solids,* Ref. 8.

[26]A. Denison, R. Ristinen, C. Zafiratos, and W. H. Tanttila (unpublished).

[27]R. van Steenwinkel and P. Zegers, Z. Naturforsch. **23a**, 818 (1968).

[28]C. Iddings and W. H. Tanttila (unpublished).

[29]George Edward Pake, *Paramagnetic Resonance* (Benjamin, New York, 1962), p. 126.

[30]R. J. C. Brown, H. S. Gutowsky, and K. Shimomura, J. Chem. Phys. **38**, 76 (1963).

[31]J. H. Van Vleck, Phys. Rev. **57**, 426 (1940); **57**, 1052 (1940). D. J. Toms and W. H. Tanttila, Phys. Status Solidi B **102**, K101 (1980), footnote 2.

[32]D. J. Toms and W. H. Tanttila, Phys. Status Solidi B **102**, K101 (1980), footnote 2.

[33]Compare this result with the same sort of conclusion for vitreous germania in our paper in Ref. 7.